POLISH MARITIME RESEARCH 3(61) 2009 Vol 16; pp. 18-25
10.2478/v10012-008-0028-2

Drag force on a flat plate in cavitating flows

M.S. Seif, Prof.
A. Asnaghi, Research Assistant
E. Jahanbakhsh, Research Assistant
Sharif University of Technology

ABSTRACT

The present study focuses on the simulation of two dimensional unsteady cavitating flows. For simulation of unsteady behaviors of cavitation which have practical applications, the development of unsteady PISO algorithm based on the non-conservative approach is utilized. For multi-phase simulation, single-fluid Navier–Stokes equations, along with the volume fraction transport equation, are employed. The bubble dynamics model is utilized to simulate phase change between vapor and liquid phases of the water. Unsteady simulation of cavitation around NACA66(MOD) and supercavitation around a flat plate normal to flow direction are performed to clarify accuracy of presented model. Numerical results and comparisons with experimental data are provided. The accuracy is good, and it is possible to apply this method to more complex shapes.

Keywords: numerical simulation; cavitation; psio algorithm; flat plate; unsteady flow

INTRODUCTION

When local static pressure of liquid falls below the corresponding saturated pressure, the phase of fluid changes from liquid into vapor. This phenomenon is named cavitation. The cavitation is departure from evaporation. The evaporation, in definition, is performed by temperature changing but cavitation is performed by pressure changing. Cavitation can be observed in a wide variety of propulsion and power systems like propellers, pumps, nozzles and injectors [1, 2].

Cavitation is categorized by a dimensionless number called cavitation number, where it depends on the saturated pressure, the flow reference pressure, density and velocity, respectively. The cavitation number is defined as follows:

$$\sigma = \frac{P - P_{sat}}{\frac{1}{2}\rho_{\infty} U_{\infty}} \tag{1}$$

Usually cavitation formation of a flow is categorized based on the cavitation number of the flow. Therefore, experimental observations are classified based on the cavitation number of the flow [3]. Undesirable aspects of cavitation are erosion, structural damages, noise and power loss in addition to beneficial features such as drag reduction and the effects of cavitation in water jet washing systems. The drag reduction observed on bodies surrounded fully or partially with cavity strongly encourages one to research on properties of cavitating flows.

In spite of its longstanding practical importance and rich physics, cavitating flow continues to be a topic of significant challenge to the computational community. The simultaneous presence of interfacial dynamics, multiple timescales, and phase change complicates the fluid physics and requires substantial modeling efforts. Numerous modeling strategies have been proposed in the literature, ranging from Rayleigh-Plesset type of bubble formulation, Kubota et al. [4], which separates the liquid and vapor region based on the force balance notion, to homogeneous fluid approach, Senocak and Shyy [5], which treats the cavity as a region consisting of continuous composition of liquid and vapor phases.

In this study the bubble dynamic model which is based on the Rayleigh equation is used for simulating phase change. A finite-volume approach written in body fitted curvilinear coordinates, on collocated grids in 2D and 3D domains is used for the numerical descretization. For the present study, the transport equation-based model, TEM, is implemented into the solver and related modifications, regarding the convection schemes and the PISO algorithm, have been made for time-dependent computations.

The main numerical results of this study are from simulation of sheet cavitation around NACA66(MOD) hydrofoil and supercavitation around a flat plate. Unsteady simulation of cavitating flows around a 2d flat plate oriented normal to flow is performed from range of subcavitation to supercavitation. Apart from their theorical interest (in stability analysis for instant), unsteady supercavitating flows were mainly considered in the past for their applications to hydrofoils under transient or periodic conditions. On the whole, the basis of the modeling of unsteady 2d supercavities is the same as for steady flows.

The main analysis methods are:

1. analytical, non-linear methods: Von Karman [6], Woods [7], Wu [8]
2. analytical, linearized methods: Timmam [9], Geurst [10], Tuln et al. [11]
3. numerical, non-linear methods, which are currently employed and usually use the scheme initially proposed by Plesset et al. [12]. A survey of numerical techniques for unsteady cavity flow modeling was given by Kinnas [13].

Due to the difficulty of conducting tests under unsteady conditions, experimental data in this field are rather rare. Therefore, the published experimental results usually consist of time-averaged properties [14].

The simulated flows around the flat plate consist of unsteady cavitating flows from two-phase vortex shedding to fully supercavitating flows. Based on these simulations, the pressure distribution, cavity region, cavity characters as its length and width are presented. Beside these, the interaction between vapor phase and flow around the flat plate, formation of supercavitation and its effects are analyzed. Finally, the obtained results are compared with available experimental results to demonstrate the accuracy of the current simulation.

GOVERNING EQUATIONS

The equations governing the flow of a compressible fluid are the continuity equation, the momentum equations, the energy equation, and finally the state equation. This set of non-linear, coupled equations is solved for the unknown's parameters ρ, U, T and P. In index notation form, these equations may be written as:

$$\frac{\partial \rho_m}{\partial t} + \frac{\partial (\rho_m u_i)}{\partial x_i} = 0 \tag{2}$$

$$\frac{\partial (\rho_m u_i)}{\partial t} + \frac{\partial (\rho_m u_i u_j)}{\partial x_j} = \tag{3}$$

$$= -\frac{\partial (P)}{\partial x_i} + \frac{\partial}{\partial x_j}\left(\mu \left(\frac{\partial u_i}{\partial x_j} + \frac{\partial u_j}{\partial x_i} \right) \right) + \rho_m g$$

$$\frac{\partial (\rho_m T)}{\partial t} + \frac{\partial (\rho_m u_j T)}{\partial x_j} = \tag{4}$$

$$= \frac{1}{C_P}\left(\frac{\partial}{\partial x_j}\left(K \frac{\partial T}{\partial x_j} \right) + \beta T \left[\frac{\partial P}{\partial t} + u_j \frac{\partial P}{\partial x_j} \right] + \dot{\varphi} + \dot{q} \right)$$

Where $\dot{\varphi}$ denotes the dissipation term in energy equation and β is the thermal expansion coefficient which is equal to 1/T for an ideal gas. In addition to the above differential equations, an auxiliary equation of state relating density to pressure and temperature [ρ = f(P,T)] is needed. In many practical problems related to cavitation phenomena, the change in temperatures is negligible. Therefore the simulation of cavitation in isothermal condition has not any effect on final results, and it is unnecessary to solve the energy equation. Therefore the pressure-density coupling is complex and requires special attention [15].

In this study, instead of a state equation, the TEM of vapor is employed. With this equation, pressure and density are connected implicitly via a phase change source term. To simulate phase change between vapor and liquid, a term S_α, is added to the right side of vapor volume fraction equation. The vapor volume fraction equation with the phase change source term in its right side is presented in equation (5).

$$\frac{\partial \alpha_v}{\partial t} + \frac{\partial (\alpha_v u_i)}{\partial x_i} = S_\alpha \tag{5}$$

The source term of the vapor volume fraction equation presents the rate of phase change between vapor and liquid phases. The utilized phase change model is presented in the part of cavitation model.

The Homogenous model

With determination of the volume of fraction, the local properties of fluid can be achieved based on the single state of each phase. This method is named The Homogenous model. In two phase flows, the mixture density and mixture viscosity are defined as follows based on the vapor volume fraction:

$$\begin{aligned} \rho_m &= \alpha_v \rho_v + (1-\alpha_v)\rho_l \\ \mu_m &= \alpha_v \mu_v + (1-\alpha_v)\mu_l \end{aligned} \tag{6}$$

Cavitation model

In TEM approach, numerical models of cavitation differ in cavitation source term, S_α . The cavitation source term defines vapor net mass generation that contains effects of vapor production and destruction. In this study we consider the bubble dynamics method as the phase change model [16, 17]. Therefore S_α may be written as:

$$S_\alpha = \mathrm{sign}(P_{sat} - P) \frac{n_0}{1 + n_0 \frac{4}{3}\pi R^3} 4\pi R^2 \sqrt{\frac{2|P_{sat} - P|}{3\rho_l}} \tag{7}$$

The average nucleus per liquid volume is considered as $n_0 = 10^8$. Other properties such as the minimum radius of bubble can be calculated based on the value of the n_0 [18].

DISCRETIZATION METHOD

A finite volume method is used to discretize the governing equations. The details related to the finite volume discretization methods of the Navier Stokes equations and the conservation of mass equation can be found in different references [19].

Equations descretization

In the descretized form of Navier-Stokes equations, there are three major terms: the unsteadiness, convection and diffusion terms. The discretization of the diffusion flux does not require any special consideration and the method adopted here is the second order estimation. The discretization of the convection flux is, however, problematic and requires special attention. In this study, the First-Order Upwind (FOU) scheme is used to calculate the faces values. However, for increasing the solution stability, high order methods could be utilized such as Jassak method [20]. For the representation of the unsteady term, the time derivative is approximated using the First-Order Euler-implicit formulation [16, 20].

To discretize the volume of fraction transport equation, it is necessary to compute the values on the computational cells interfaces accurately. In high speed flows and for capturing shock, it is necessary to use high order methods such as

HRIC [21, 22]. In low speed flows, the first order Upwind method can be used to calculate the volume fraction values on computational cells faces [15]. With the homogeneous approach and volume fraction values on faces, the density on the cell interface can be calculated.

The velocity fluxes on computational cells faces are calculated by using momentum interpolation. The momentum interpolation avoids pressure oscillations in the solution procedure [21].

Overall Solution Procedure

Selecting a suitable time step for unsteady simulation of cavitating flows is very important. The selected time step should be proper for convection in the vapor transport equation and the continuity equation, as well as Navier-Stokes equations. If the time step is selected inappropriately, final results may be wrong or the solution procedure may diverge. In some researches, the time step is considered in accordance with the non-dimensional time of the flow. The non-dimensional time is obtained by dividing the length scale to reference velocity of the flow [23]. In another approach, the time step is calculated in the beginning of each time step by considering the courant number, CFL [18]. In this study, the CFL parameter is used to calculate the time step.

After calculating suitable time step, it is possible to start the solution procedure. For each time step, first, the vapor fraction transport equation is solved and a new vapor fraction distribution is obtained. Consequently the values of the mixture density and viscosity are updated. Based on these new values, the Navier-Stoks equations and the pressure correction equations are solved until a convergence criterion is reached. Then, the whole procedure is repeated within the next time step. In this study, for solving velocity-pressure coupling, the non-conservative PISO algorithm is used.

For the numerical simulation of cavitating flows, the pressure level usually is defined by a pressure boundary condition at the outlet of the computational domain, and velocity set as an inlet velocity boundary.

NUMERICAL RESULTS

The numerical model was implemented in the CFD-Code developed at the Marine Engineering Lab. of Sharif University of Technology. The accuracy of this software are evaluated through different numerical simulations.

The flow is assumed isothermal and fluid properties are supposed to be constant at a given temperature for the entire flow domain. For all simulations presented, cold water at a constant temperature T = 293.2 K with 10^8 nuclei per m^3 water having a minimal nuclei radius of 30 microns is assumed to match the experimental conditions. The saturated pressure, P_v, is set to a constant value of 2340 Pa.

NACA66(MOD) Hydrofoil

Effects of leading edge cavitation on NACA66(MOD) were experimentally investigated by Shen and Dimotakis [24]. A 2D NACA66(MOD) airfoil with camber ratio of 0.02, mean line of 0.8 and thickness ratio of 0.09 is used in this simulation. The implied boundary conditions and non-orthogonal meshes are shown in Fig. 1.

The published experimental results contain the distribution of static pressure on hydrofoil surface at different angles of attack and Reynolds numbers. In this study, Leading Edge Cavitation simulations were performed at Re = 2×10^6, an angle of attack of 4 deg, inlet velocity 2.5 m/s and cavitation number of 0.91; under these conditions, the cavitation is confined to the front of the hydrofoil. Calculated Cp values, equation (8), on hydrofoil top surface are shown in Fig. 2 together with experimental data, and good correlation is clear between these results. The vapor volume fraction distribution is shown in Fig. 3, which shows the cavitation zone on the hydrofoil surface.

$$C_p = \frac{P_\infty - P}{\frac{1}{2}\rho_\infty U_\infty^2} \tag{8}$$

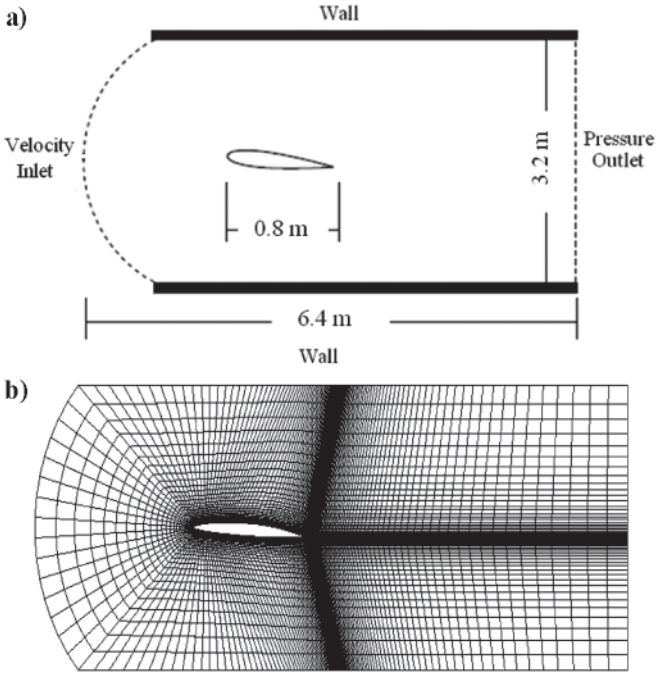

*Fig 1. Implied boundary conditions (**a**) and non-orthogonal meshes (**b**) for simulation of cavitation around NACA66(MOD)*

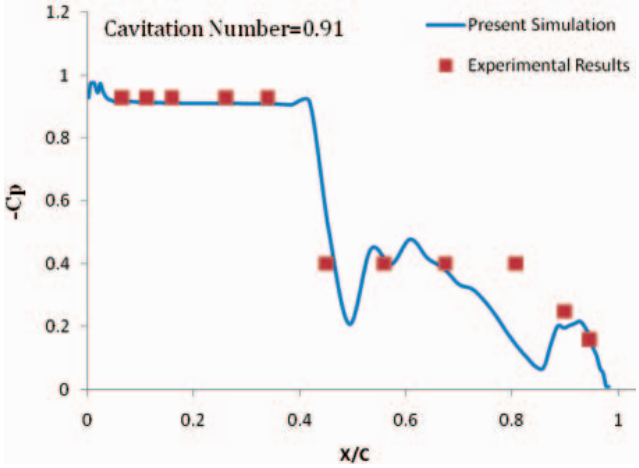

Fig. 2. Comparison between obtained numerical pressure coefficient distribution and Experimental Results[5] around NACA66(MOD), Inlet velocity = 2.5 m/s. Outlet cavitation number = 0.91

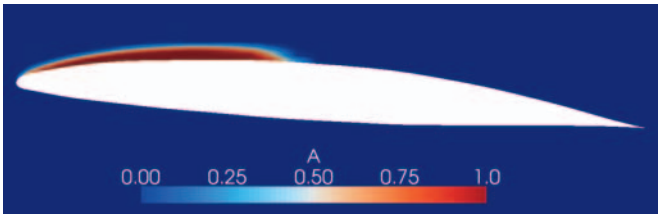

Fig. 3. Vapor volume fraction distribution around NACA66(MOD), Inlet velocity = 2.5 m/s. Outlet cavitation number = 0.91

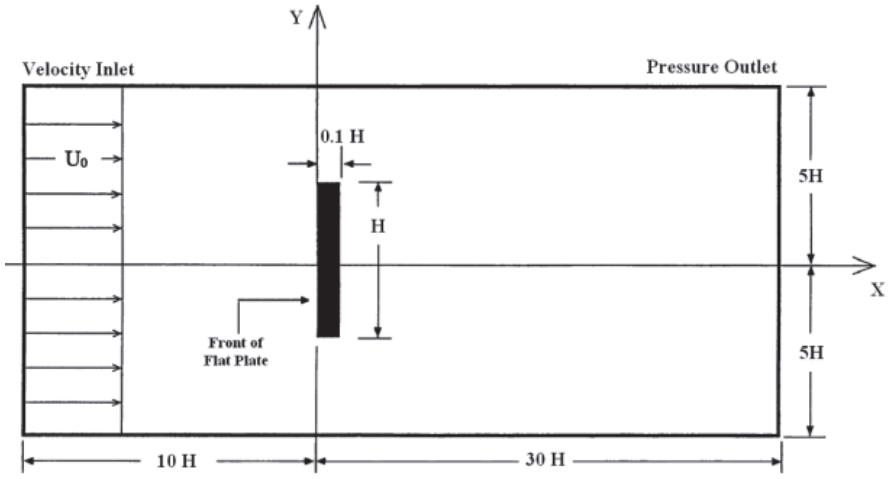

Fig. 4. Implied computational domain, boundary conditions and coordinate system for simulation of cavitation around the flat plate

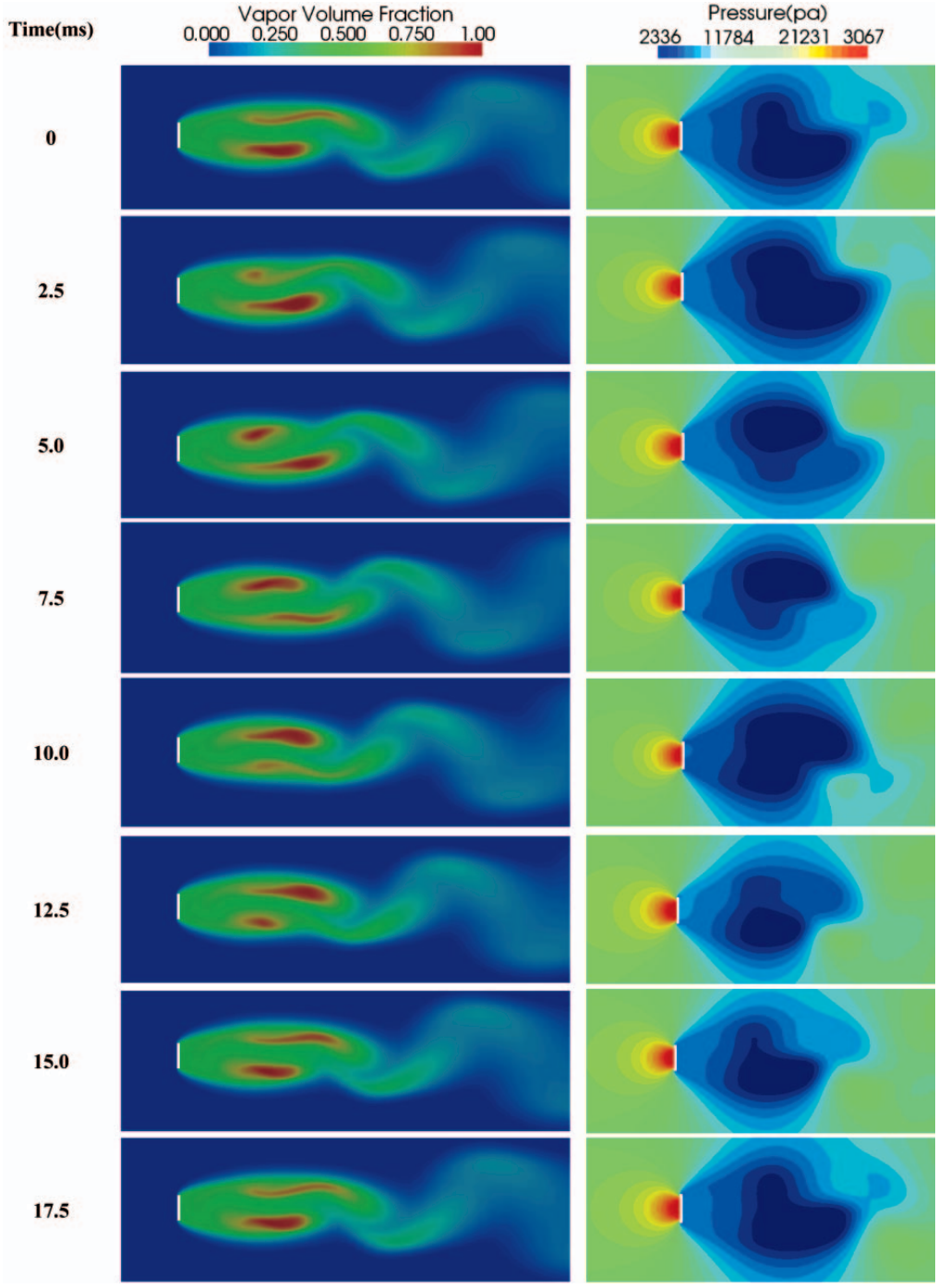

Fig. 5. Vapor volume fraction and pressure distribution around the flat plate Inlet velocity = 5 m/s. Outlet cavitation number = 1.0

Flat Plate

Geometry and Boundary Conditions

The used computational domain and geometry are presented in Fig. 4. The plate has height H and thickness 0.1H where H is equal to 0.1 m. The boundaries of upstream and downstream are located at 10H and 30H. The upper and lower boundaries are located at 5H from the center of plate. The constant velocity inlet and constant pressure outlet are considered as inlet and outlet boundaries. The main results are obtained by considering outlet cavitation number equal to 1.0 and 1.25, and velocity inlet equal to 5m/s.

Unsteady behavior of cavitation

For considering unsteady behavior of fully cavitating flows behind the flat plate, the formation of cavitation and its oscillations are presented in Fig. 5. The considered cavitation number is equal to 1.0 at the outlet boundary. As presented in Fig. 5, supercavitation is formed behind the flat plate in these conditions. At the end of this cavity, the two phase vortex shedding occurs, and vapor is separated from cavity by vortexes and moved to the down stream. The cycle of this separation occurs in 17.5 ms. Therefore, the frequency is equal to 57.14 Htz. Along with the vapor contours, pressure contours are presented in Fig. 5, which shows the same oscillating behavior.

Cavity Dimensions

One of the most important characters of supercavitating flows is their cavity dimensions. The cavity dimensions are usually normalized by the height of the flat plate. The vapor iso-surfaces are presented in Fig. 6. In this figure, one snapshot of periodic behaviors of each cavitation number is presented. By using these vapor iso-surfaces, average cavity length and width can be estimated. Besides, non-dimensional cavity length and width are presented in Fig. 7 and Fig. 8. At the small values of cavitation number, most of the flow domain contains vapor phase. In these situations, the re-entrant jet and vapor volume fraction distributions inside the cavity are much more complicated than sub-cavitation flows. The obtained results for cavity dimensions are compared with experimental results reported by Waid [25]. One of the basic objectives of this paper is to improve simulation of supercavitating flows. For this reason, the obtained results are also compared with other numerical simulations [26]. By this comparison, it is clear that the implied method improves accuracy of supercavitation simulations considerably.

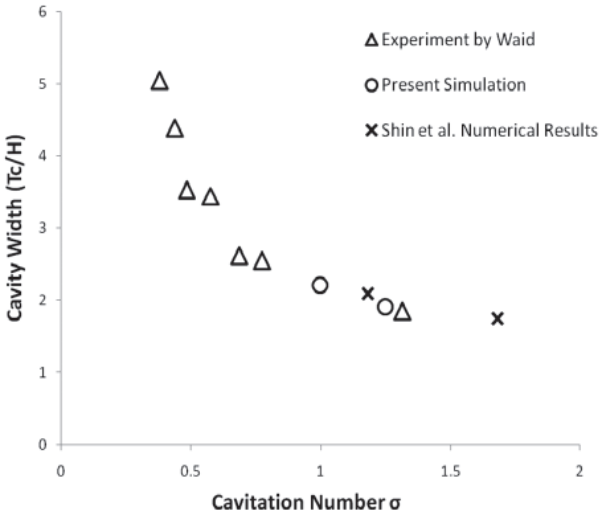

Fig. 7. *Cavity width defined by α = 0.5 for several cavitation number Experimental data by Waid [25], Shin et al. numerical results[26]*

Drag Forces

Drag force variation is another important character of cavitating flows. In the flow around of the flat plate, drag force is mainly pressure drag force. The average pressure distributions around the flat plate is presented in Fig. 9. By integrating these pressure distributions, average drag forces can be obtained.

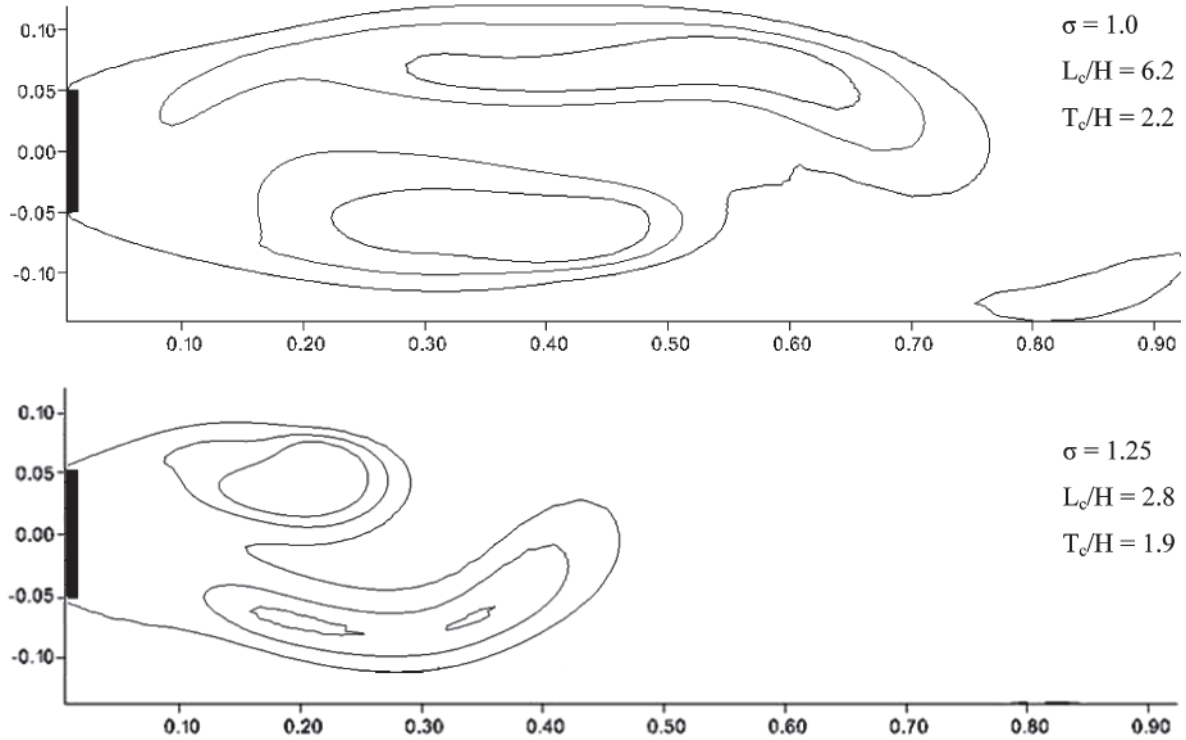

Fig. 6. *Vapor volume fraction Iso-surface and cavity dimensions around the flat plate Inlet velocity = 5 m/s, Outlet cavitation number = 1.0, 1.25*

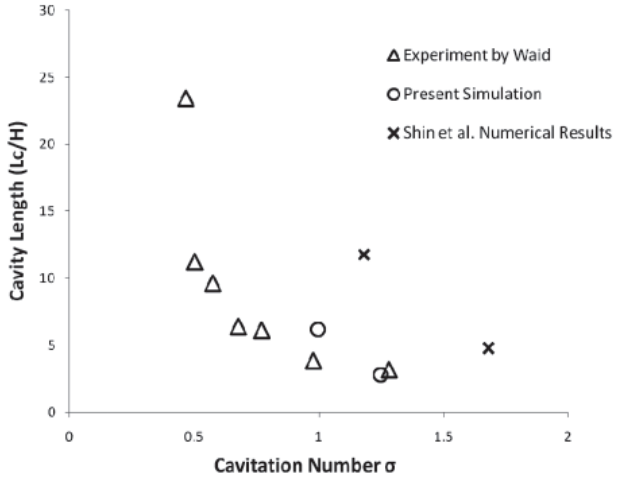

Fig. 8. Cavity length defined by α = 0.5 for several cavitation number Experimental data by Waid [25], Shin et al. Numerical results[26]

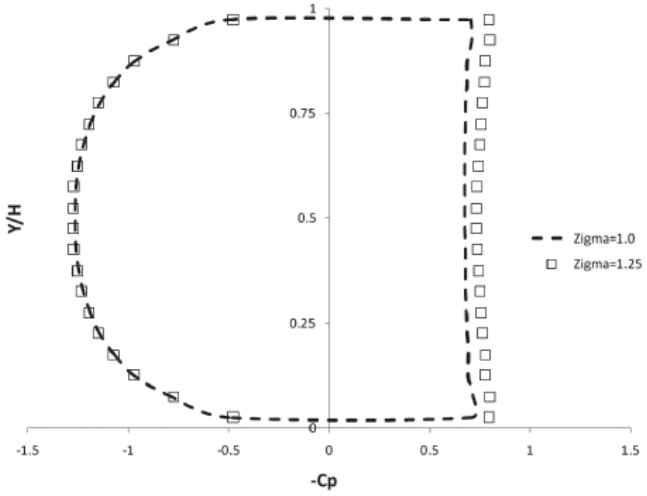

Fig. 9. Average pressure coefficient distribution of the 2d flat plate for several cavitation number

In the flow around the flat plate, the drag force consists of the front force implied in the front of plate, and the back force. In the Fig. 10, the unsteady behavior of these two drag forces, and total drag force are presented for one cycle. From this figure, it is obvious that variations of these forces are similar. The average forces for the front and back of the plate, and also the total drag force can be obtained from this figure. By using the average of the total drag force, part (c) of Fig. 10, and the reference velocity and density values, the average drag coefficient can be calculated. In the Fig. 11, variations of average drag coefficient against cavitation number are presented. In this figure, the free stream prediction [12], Shin et al. numerical results [26] and experimental results by Waid [25] are presented together with present numerical results.

Beside the undesirable aspects of cavitating flows such as noise and erosion, the developed cavity can reduce drag forces, especially in supercavitating flows. This beneficial aspect of cavitating flows can help to increase the velocity of vehicles in constant power. When speed of vehicle isn't enough to create supercavitation naturally, Ventilation can be used to create or to enhance a supercavity called ventilated cavitation. In the Fig. 11, it is presented that by development of cavitation and reduction of cavitation numbers of the flow, drag force reduces. The summery of obtained numerical results for simulation of cavitation around the flat plate are presented in Tab. 1.

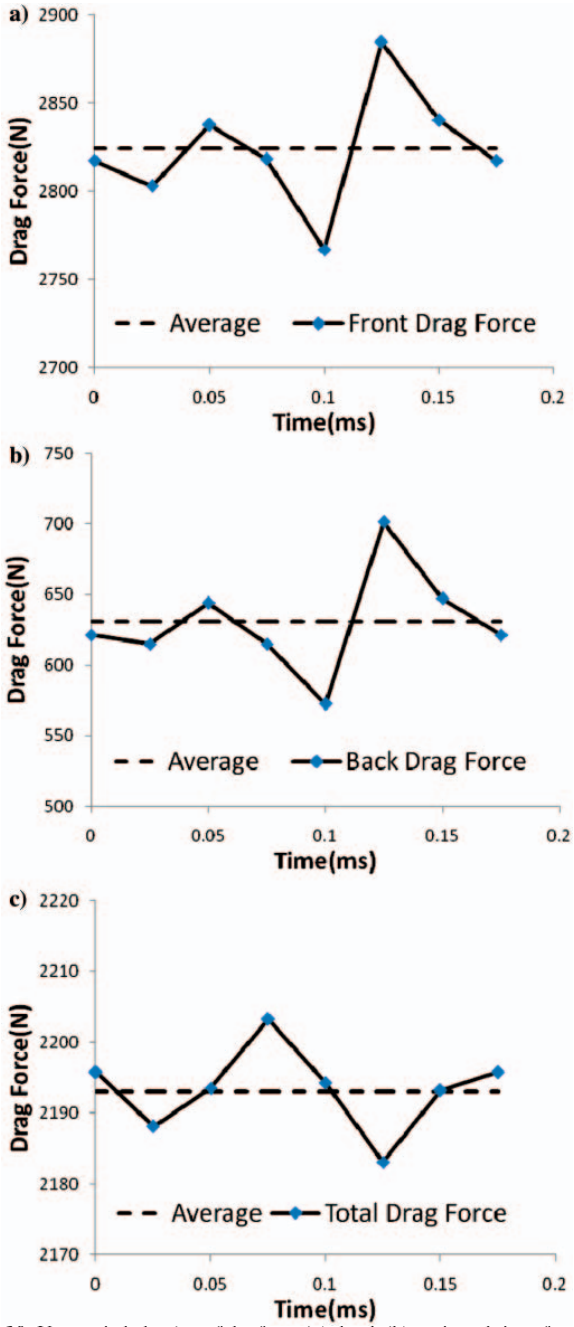

Fig. 10. Unsteady behavior of the front (a), back (b) and total drag force (c) of the 2d flat plate Inlet velocity = 5 m/s, Outlet cavitation number = 1.0

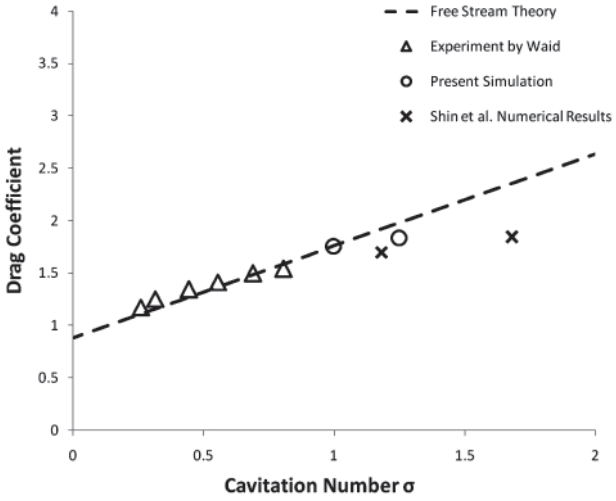

Fig. 11. Average drag coefficient of the 2d flat plate for several cavitation number Experimental data by Waid [25], Shin et al. Numerical results[26], Free Stream Theory[12]

Tab. 1. The summery of obtained results for simulation of cavitation around the flat plate

σ	Re_∞	L_c/H	T_c/H	Ave. Drag Force (N)	Ave. Drag Coefficient
1.0	5×10^5	6.2	2.2	2193	1.75
1.25	5×10^5	2.8	1.9	2888	1.83

Tab. 2. The comparison between cavitating and non-cavitating simulation results

	Cavitation Simulation Results		Non-Cavitation Simulation Results	
σ	Ave. Drag Force (N)	Ave. Drag Coefficient	Ave. Drag Force (N)	Ave. Drag Coefficient
1.0	2193	1.75	3903	3.12

It seems necessary to estimate gain accuracy via simulation of cavitation in a flow. For this reason, the simulated cavitating flows are compared with results of non-cavitating simulations. This comparison shows simulation of cavitation can provide more accurate results for drag force, periodic behavior, and pressure distributions. The comparison between caviatiting numerical results and non-cavitating numerical results are presented in Tab. 2.

CONCLUSIONS

- Unsteady simulations have been performed for 2D cavitating flows. For phase change modeling, the Bubble dynamics cavitation model is utilized, which is presented as the source terms in the volume of fraction equation and the continuity equation. The non-conservative PISO method is used to solve coupling between the continuity and N.S. equations. Unsteady behavior of cavitation around a flat plate oriented normal to flow direction, and sheet cavitation around a NACA66(MOD) hydrofoil are performed to demonstrate the accuracy of the selected algorithm.

- Based on the implied phase change model, the supercavitating flow behind the flat plate has been simulated in a good agreement with the experimental results. The size of the vapor region and the separation of the cavitation are clearly predicted by the developed CFD-code. These predictions provide information that will be helpful for understanding behaviors of unsteady cavity flows such as cavitation occurrence and development. The effects of vapor generation on drag reduction are investigated and presented. It is presented that by growth of cavity and reduction of cavitation number, the drag force reduces.

- The results of the unsteady simulation show the development of a re-entrant jet and two-phase vortex shedding. The predicted cavity dimensions, drag coefficients and pressure distributions show a very good agreement with the experiments.

NOMENCLATURE

C – hydrofoil chord
CFL – courant number
C_p – pressure coefficient
g_i – gravity
H – plate height
K – termal expansion coefficient
L_c – cavity average length
n_0 – average nucleus per liquid volume
P – pressure
P_{sat} – saturation pressure
$\dot{q}$ – energy source term
R – gas constant (eq. ())
R – nucleus radius
Re – reynolds number
S_α – vapor phase change term
t, t_∞ – time, mean flow time scale
T – temperature
T_c – cavity maximum thickness
u_i – cartesian velocity components
U – velocity
x_i – cartesian coordinates

α – volume fraction
β – termal expansion coefficient
σ – cavitation parameter
$\dot{\varphi}$ – energy dissipation term
μ – viscosity
ρ – density

subscripts, superscripts
∞ – free stream
m – mixture
l – liquid phase
v – vapor phase
sat – saturation condition
i, j – coordinate indices

BIBLIOGRAPHY

1. Wiesche S.: *Numerical simulation of cavitation effects behind obstacles and in an automotive fuel jet pump*, Heat Mass Transfer, 2005.
2. Frobenius M. and Schilling R.: *Three-Dimensional unsteady cavitating effects on a single hydrofoil and in a radial pump-measurement and numerical simulation*, Cav03-GS-9-005, Proceedings of the 5th international symposium on cavitation, Osaka, 2003.
3. Singhal A.K., Vaidya N. and Leonard A.D.: *Multidimensional simulation of cavitating flows using a PDF model for phase change*, ASME Fluids Engineering Division Summer Meeting, ASME Paper FEDSM97-3272, 1997.
4. Kubota A., Kato H., Yamaguchi H.: *A New Modeling of Cavitating Flows: A Numerical Study of Unsteady Cavitation on a Hydrofoil Section*. J. Fluid Mech. 1992
5. Senocak I., Shyy W.: *Evaluation of cavitation models for Navier-Stokes computations*, Proceeding of FEDSM 02, ASME fluid engineering division summer meeting, Montreal, Canada, 2002

6. Von Karman T.: *Accelerated flow of an incompressible fluid with wake formation*, Ann. Mathem. Pura Applic. IV(29), 1949
7. Woods L.C.: *Unsteady plane flow past curved obstacle with infinite wakes*. Proc. Roy. Soc. A 229, 1955
8. Wu T.Y.T.: *Unsteady supercavitating flows*. Proc. 2nd Int. Symp. on Naval Hydrodynamics, 1958
9. Timmam R.: *Ageneral linearized theory for cavitating hydrofoils in non steady flow*. Proc. 2nd Int. Symp. on Naval Hydrodynamics, 1958
10. Geurst J.A.: *Some investigations of a linearized theory for unsteady cavity flows*. Arch. Rat. Mech. Anal. 5(4), 1960.
11. Tulin M.P., Hsu C.C.: *New applications of cavity flow theory*. Proc. 13th Int. Symp. on Naval Hydrodynamics, Tokyo, 1980
12. Knapp R.T., Daily J.W., Hammitt F.G.: *Cavitation*. McGraw-Hill Book Co, New York, 1970
13. Kinnas S.A.: *The prediction of unsteady sheet cavitation*. Proc. 3rd Int. Symp. on Cavitaton, Vol. 1, Grenoble(France), 1998
14. Franc J.P., Michel J.M.: *Fundamental of cavitation*, Kluwer Academic Publishers, 2004.
15. Moukalled F. and Darwish, M.: *A Unified Formulation of the Segregated Class of Algorithms for Fluid Flow at All Speeds*, Numer. Heat Tr. B-Fund, 37, 2000
16. Delannoy Y., Kueny J.L.: *Two-phase flow approach in unsteady cavitation modelling*. Cavitation and Multiphase Flow Forum, FED ASME 98, 1990
17. Sauer J.: *Instationär kavitierende Strömungen - Ein neues Modell, basierend auf Front Capturing (VoF) und Blasendynamik*. Universität Karlsruhe, 2000
18. Senocak I., and Shyy W.: *Numerical Simulation of Turbulent Flows with Sheet Cavitation*, CAV2001, Proc. 4th International Symposium on Cavitation, CAV2001A7.002, California Institute of Technology, Pasadena, CA, 2001
19. Jahanbakhsh E., Panahi R. & M.S. Seif: *Numerical Simulation of Three-Dimensional Interfacial Flows*, International Journal of Numerical Methods for Heat & Fluid Flow, Issue 4, 2007
20. C.M. Rhie and W.L. Chow: *Numerical study of the turbulent flow past an airfoil with trailing edge sepration*, AIAA J, 1525, 1983
21. Issa, R.I.: *Solution of the Implicitly Discretized Fluid Flow Equations by Operator-Splitting*, J. Comput. Phys., 62, 1985
22. Kunz R.F., Boger D.A., Stinebring D.R., Chyczewski T.S., Lindau J.W., Gibeling H.J., Venkateswarn S., Govindan T.R.: *A pre Preconditioned Navier–Stokes method for two-phase flows with application to cavitation prediction*. Computers & Fluids, 2000
23. Shen Y. J. and Dimotakis P. E.: *The Influence of Surface Cavitation on Hydrodynamic Forces*, Proc. 22nd ATTC, St. Johns, 1989
24. Waid RL: *Water tunnel investigation of two-dimensional cavities*. In: Knapp RT, Daily JW, Hammitt FG (eds) Cavitation. McGraw-Hill Book Co, New York, 1957
25. Shin B.R., Iwata Y., Ikohagi T.: *Numerical simulation of unsteady cavitating flows using a homogenous equilibrium model*, J. Comput. Mechanics. 2003

CONTACT WITH THE AUTHORS
M.S. Seif, Prof.
A. Asnaghi, Research Assistant,
E. Jahanbakhsh, Research Assistant,
Sharif University of Technology
11155-9567, Azadi Avenue,
Tehran, IRAN
email: seif@sharif.edu